



Title	Substrate recognition of the catalytic $\alpha$ -subunit of glucosidase II from <i>Schizosaccharomyces pombe</i>
Author(s)	Okuyama, Masayuki; Miyamoto, Masashi; Matsuo, Ichiro; Iwamoto, Shogo; Serizawa, Ryo; Tanuma, Masanari; Ma, Min; Klahan, Patcharapa; Kumagai, Yuya; Tagami, Takayoshi; Kimura, Atsuo
Citation	Bioscience biotechnology and biochemistry, 81(8), 1503-1511 <a href="https://doi.org/10.1080/09168451.2017.1320520">https://doi.org/10.1080/09168451.2017.1320520</a>
Issue Date	2017-08
Doc URL	<a href="http://hdl.handle.net/2115/71180">http://hdl.handle.net/2115/71180</a>
Rights	This is an Accepted Manuscript of an article published by Taylor & Francis in Bioscience biotechnology and biochemistry on 2017 Aug, available online: <a href="http://www.tandfonline.com/10.1080/09168451.2017.1320520">http://www.tandfonline.com/10.1080/09168451.2017.1320520</a> .
Type	article (author version)
File Information	text_170411.pdf



[Instructions for use](#)

***Regular paper***

Title

**Substrate recognition of the catalytic  $\alpha$ -subunit of glucosidase II from *Schizosaccharomyces pombe***

Authors

Masayuki Okuyama<sup>1,†,\*</sup>, Masashi Miyamoto<sup>1,†</sup>, Ichiro Matsuo<sup>2</sup>, Shogo Iwamoto<sup>2</sup>, Ryo Serizawa<sup>1</sup>, Masanari Tanuma<sup>1</sup>, Min Ma<sup>1</sup>, Patcharapa Klahan<sup>1</sup>, Yuya Kumagai<sup>1</sup>, Takayoshi Tagami<sup>1</sup> and Atsuo Kimura<sup>1,\*</sup>

<sup>1</sup> *Research Faculty of Agriculture, Hokkaido University, Sapporo 060-8589, Japan.* <sup>2</sup> *Graduate School of Science and Technology, Gunma University, Kiryu 376-8515, Japan.*

Email addresses

MO, okuyama@abs.agr.hokudai.ac.jp; MM, masashi.m1229@gmail.com; IM, matsuo@gunma-u.ac.jp; SI, t11802104@gunma-u.ac.jp; RS, ryo.serizawa@frontier.hokudai.ac.jp; MT, tanuma.marbo.0415@gmail.com; MM, mamin@abs.agr.hokudai.ac.jp; PK, patchakl@abs.agr.hokudai.ac.jp; YK, ykumagai@abs.agr.hokudai.ac.jp; TT, tagami@abs.agr.hokudai.ac.jp; AK, kimura@abs.agr.hokudai.ac.jp

Running title

Substrate recognition of catalytic subunit of ER GII

\*Corresponding authors: E-mail, kimura@abs.agr.hokudai.ac.jp. (AK);

Email: okuyama@abs.agr.hokudai.ac.jp (MO)

†The first two authors contributed equally to this work.

Funding

This work was supported by JSPS KAKENHI Grant Numbers 22780082 and 26450114.

## 1 **Abstract**

2       The recombinant catalytic  $\alpha$ -subunit of *N*-glycan processing glucosidase II from  
3 *Schizosaccharomyces pombe* (SpGII $\alpha$ ) was produced in *Escherichia coli*. The recombinant  
4 SpGII $\alpha$  exhibited quite low stability, with a reduction in activity to < 40% after 2-days  
5 preservation at 4°C, but the presence of 10% (v/v) glycerol prevented this loss of activity.  
6 SpGII $\alpha$ , a member of the glycoside hydrolase family 31 (GH31), displayed the typical  
7 substrate specificity of GH31  $\alpha$ -glucosidases. The enzyme hydrolyzed not only  $\alpha$ -(1→3)- but  
8 also  $\alpha$ -(1→2)-,  $\alpha$ -(1→4)- and  $\alpha$ -(1→6)-glucosidic linkages, and *p*-nitrophenyl  $\alpha$ -glucoside.  
9 SpGII $\alpha$  displayed most catalytic properties of glucosidase II. Hydrolytic activity of the  
10 terminal  $\alpha$ -glucosidic residue of Glc<sub>2</sub>Man<sub>3</sub>-Dansyl was faster than that of Glc<sub>1</sub>Man<sub>3</sub>-Dansyl.  
11 This catalytic  $\alpha$ -subunit also removed terminal glucose residues from native *N*-glycans  
12 (Glc<sub>2</sub>Man<sub>9</sub>GlcNAc<sub>2</sub> and Glc<sub>1</sub>Man<sub>9</sub>GlcNAc<sub>2</sub>) although the activity was low.

13 **Key words:** catalytic  $\alpha$ -subunit of ER glucosidase II; heterologous expression; glycoside  
14 hydrolase family 31; substrate specificity

## 15 **Abbreviations**

16 cleavage-1, conversion of G2M9 to G1M9; cleavage-2, conversion of G1M9 to M9; BSA,  
17 bovine serum albumin; ER, endoplasmic reticulum; GH31, glycoside hydrolase family 31;  
18 GI, glucosidase I; GII, glucosidase II; GII $\alpha$ ,  $\alpha$ -subunit of glucosidase II; GII $\beta$ ,  $\beta$ -subunit of  
19 glucosidase II; G1M3, Glc<sub>1</sub>Man<sub>3</sub>; G2M3, Glc<sub>2</sub>Man<sub>3</sub>; G1M9, Glc<sub>1</sub>Man<sub>9</sub>GlcNAc<sub>2</sub>; G1M9-PA,  
20 pyridylaminated G1M9; G2M9, Glc<sub>2</sub>Man<sub>9</sub>GlcNAc<sub>2</sub>; G3M9, Glc<sub>3</sub>Man<sub>9</sub>GlcNAc<sub>2</sub>; G3M9-PA,  
21 pyridylaminated G1M9; HPLC, high-performance liquid chromatography; IPTG, isopropyl  
22  $\beta$ -thiogalactopyranoside; M9, Man<sub>9</sub>GlcNAc<sub>2</sub>; pNPG, *p*-nitrophenyl  $\alpha$ -glucopyranoside; ScGI,  
23 glucosidase I of *Saccharomyces cerevisiae*; SpGII $\alpha$ ,  $\alpha$ -subunit of glucosidase II of  
24 *Schizosaccharomyces pombe*.

## 25 **Introduction**

26        Secretory proteins of eukaryotic cells are *N*-glycosylated in the endoplasmic reticulum  
27 (ER). *N*-Glycosylation is initiated with the transfer of the precursor glycan,  
28  $\text{Glc}_3\text{Man}_9\text{GlcNAc}_2$  (G3M9), to an Asn residue in the motif Asn-Xaa-Ser/Thr of nascent  
29 polypeptides. Mannoses in G3M9 are organized in a 3'-trimannosyl branch (arm A) and a 6'-  
30 pentamannosyl branch (composed of arms B and C), with the former type capped by three  
31 glucose residues. While still in ER, terminal glucoses in arm A and mannose in arm B are  
32 removed by glycosidases. The removal of glucose residues is catalyzed by glucosidases I and  
33 II (GI and GII, respectively), and the removal of the mannose residue is catalyzed by ER  
34 mannosidase. GI specifically trims the outermost  $\alpha$ -(1→2)-linked glucose residue of G3M9  
35 to produce  $\text{Glc}_2\text{Man}_9\text{GlcNAc}_2$  (G2M9). Subsequently, GII removes a further two  $\alpha$ -(1→3)-  
36 linked glucose residues in succession: cleavage-1, conversion from G2M9 to  
37  $\text{Glc}_1\text{Man}_9\text{GlcNAc}_2$  (G1M9); and cleavage-2, conversion from G1M9 to  $\text{Man}_9\text{GlcNAc}_2$  (M9).  
38 These cleavage processes by GII have important implications for folding and quality control  
39 of nascent glycoproteins.<sup>1)</sup>

40        GII is a heterodimeric protein composed of tightly bound  $\alpha$ - and  $\beta$ -subunits (GII $\alpha$  and  
41 GII $\beta$ , respectively). GII $\alpha$  is the catalytic subunit and displays significant amino acid sequence  
42 similarity to glycoside hydrolase family 31 (GH31)  $\alpha$ -glucosidases. GH31  $\alpha$ -glucosidases are  
43 widespread in many organisms and are believed to be involved in the degradation of starch  
44 and  $\alpha$ -glucooligosaccharides (e.g., maltooligosaccharides and  $\alpha$ -glucobioses). The catalytic  
45 domain of GH31  $\alpha$ -glucosidase adopts the  $(\beta/\alpha)_8$ -barrel fold and the active site is located in a  
46 pocket at the C-terminus of the inner  $\beta$ -barrel.<sup>2-6)</sup> Recently, the three-dimensional structures  
47 of GII $\alpha$ s from *Chaetomium thermophilum* and murine were determined.<sup>7,8)</sup> The structures are  
48 almost identical to other GH31  $\alpha$ -glucosidases, except for an N-terminal segment. The  
49 structure of murine GII $\alpha$  contains a portion of the GII $\beta$ .<sup>8)</sup> This structure reveals that several

50 salt bridges and hydrogen bonds are associated with the formation of the GII heterodimer.  
51 GII $\beta$  is necessary for solubility, stability, activity and localization of GII.<sup>9,10</sup> GII $\beta$  is involved  
52 in the identification of the substrate because it recognizes the arms B and C by its mannose  
53 6-phosphate receptor homolog domain (MRH domain).<sup>11,12</sup> Structural analysis of the MRH  
54 domain of *Schizosaccharomyces pombe* GII $\beta$  indicates that a tyrosine residue is closely  
55 associated with the binding of the mannose residue.<sup>13</sup>

56 GII $\alpha$  without GII $\beta$  exhibits hydrolysis activity toward chromogenic substrates such as *p*-  
57 nitrophenyl  $\alpha$ -glucopyranoside (pNPG), but not the glucosidic residues in the physiological  
58 glycans, G2M9 and G1M9. Moreover, there are a few reports that GII $\alpha$  can trim glucose  
59 residues in native glycans without GII $\beta$ . GII $\alpha$  from *Saccharomyces cerevisiae* can catalyze  
60 cleavage-1, but not cleavage-2 without GII $\beta$ .<sup>14</sup> *S. pombe* GII $\alpha$  (SpGII $\alpha$ ) exhibits limited  
61 cleavage-1 activity *in vivo*, but not *in vitro*.<sup>12</sup> *Bombyx mori* GII $\alpha$ , a purified recombinant  
62 protein, shows weak cleavage-2 activity.<sup>15</sup> However, the detailed catalytic specificity of GII $\alpha$   
63 toward the natural *N*-glycan remains unresolved.

64 In this study, we revealed the substrate recognition of SpGII $\alpha$  for the first time by  
65 successfully obtaining soluble recombinant SpGII $\alpha$ , and the stability of recombinant SpGII $\alpha$   
66 was improved by coexistence with glycerol. Substrates used in this study were: i) substrates  
67 (maltooligosaccharides,  $\alpha$ -glucobioses, and pNPG) of GH31  $\alpha$ -glucosidases, which share the  
68 common ancestral protein with GII $\alpha$ ; ii) dansyl substrates (G2M3-Dansyl and G1M3-Dansyl)  
69 mimicking arm A of *N*-glycan; and iii) natural *N*-glycan substrates (G2M9 and G1M9).  
70 SpGII $\alpha$  hydrolyzes the substrates of GH31  $\alpha$ -glucosidase with broad specificity. Dansyl  
71 substrates and natural *N*-glycan substrates are also cleaved even without GII $\beta$ . However, the  
72 hydrolysis rate on *N*-glycan substrates is slow and this observation suggests that the assistance  
73 of GII $\beta$  is required for proper activity.

74

75 **Material and methods**

76 *Materials.* Bacto yeast extract, bacto peptone and bacto yeast nitrogen base without  
77 amino acids and ammonium sulfate were purchased from BD biosciences (Sparks, MD, USA).  
78  $\alpha,\alpha$ -Trehalose, pNPG and glycerol were from Nacalai Tesque (Kyoto, Japan). The maltose  
79 used was manufactured by Nihon Shokuhin Kako, Tokyo, Japan. Kojibiose, nigerose,  
80 maltotriose, maltotetraose, maltopentaose, maltohexaose and maltoheptaose were purchased  
81 from Wako Pure Chemical Industries (Osaka, Japan). Isomaltose was from Tokyo Chemical  
82 Industry (Tokyo, Japan). Pyridylaminated G1M9 and G3M9 (G1M9-PA and G3M9-PA) were  
83 purchased from Masuda Chemical industries Co., Ltd. (Kagawa, Japan). All chemicals used  
84 were of analytical grade unless otherwise noted.

85

86 *Strains and vectors.* *Escherichia coli* (*E. coli*) strain DH5 $\alpha$  was used for cloning, whereas  
87 BL21-CodonPlus (DE3)-RIL and -RP (Stratagene, La Jolla, CA, USA), and Rosetta™ (DE3)  
88 (Novagen-Merck Millipore, Billerica, MA, USA) were used for recombinant protein  
89 expression. *E. coli* expression vectors, pCold I DNA and pET vectors (pET23d and pET41a),  
90 were purchased from Takara Bio (Otsu, Japan) and Novagen-Merck Millipore, respectively.  
91 *S. cerevisiae* NBRC 1136 (S288C) was from the National Institute of Technology and  
92 Evaluation Biological Resource Center, Kisarazu, Japan, and *Pichia pastoris* GS115 and the  
93 pPICZ $\alpha$ A plasmid vector were from Invitrogen (Thermo Fisher Scientific, Carlsbad, CA,  
94 USA). *S. pombe* AHU 3179 was kindly supplied by the Applied Microbiology Laboratory,  
95 Research Faculty of Agriculture, Hokkaido University, Sapporo, Japan.

96

97 *Cloning of the gls2 gene and construction of its expression plasmid.* The *gls2* gene  
98 (SPAC1002.03c) encoding SpGII $\alpha$  was amplified by PCR using genomic *S. pombe* DNA as  
99 the template using the two primers (sense\_1 of 5'-TGTAACCTTCTCCCGGGAAAGATTCC-

100 3' and antisense\_1 of 5'-TTTCTCCATAAACGTTAAATATTGG-3') and thermostable KOD-  
101 plus-DNA polymerase (Toyobo, Osaka, Japan). The PCR product was cloned into pBluescript  
102 II SK(+) (Stratagene) to obtain SK-gls2. The recombinant SpGII $\alpha$  was produced as a fusion  
103 protein with a His<sub>6</sub>-affinity tag at the C-terminus as follows. DNA encoding the predicted  
104 mature SpGII $\alpha$  (Ala26 to Val923) was amplified by PCR using SK-gls2 as the template with  
105 primers: sense\_2 (5'-TGCCCCATGGCATTTCGACATCAATTTAAA-3', the *Nco*I site is  
106 underlined) and antisense\_2 (5'-AATCTCGAGAACCACAAAAAAGTTGTGGATT-3', the  
107 *Xho*I site is underlined). The presence and location of the signal peptide cleavage site was  
108 predicted by the Signal P server (<http://www.cbs.dtu.dk/services/SignalP/>).<sup>16)</sup> The PCR  
109 product was digested with *Nco*I and *Xho*I, and then introduced into the *Nco*I–*Xho*I sites of  
110 pET23d to generate the pET23d-gls2 plasmid for recombinant SpGII $\alpha$  production.

111

112 *Cloning of the CWH41 gene and construction of its expression plasmid.* The expression  
113 vector of the CWH41 gene (YGL027C) encoding *S. cerevisiae* processing glucosidase I  
114 (ScGI) was constructed according to previous reports.<sup>17,18)</sup> The enzyme was a truncated form  
115 (Glu33 to Phe833) with the N-terminal *S. cerevisiae*  $\alpha$ -factor secretion signal and a C-terminal  
116 His<sub>6</sub>-affinity tag. ScGI was produced in *P. pastoris* using pPICZ $\alpha$ A as follows. The CWH41  
117 gene was amplified by PCR using genomic *S. cerevisiae* DNA as the template with primers:  
118 CWH41\_F (5'-AAGTAGTGGATAATAACGGTTCAGG-3') and CWH41\_R (5'-  
119 CTTACTAGTAAGCGTCCAAGGATGTTGAC-3', the *Spe*I site is underlined). The  
120 insertion of *Spe*I resulted in a substitution of an amino acid residue, Phe833→Leu. Primostar  
121 Max DNA polymerase (Takara Bio) was used as the thermostable DNA polymerase. The PCR  
122 product was cloned into pBluescript II SK(+) to obtain SK-CWH41. SK-CWH41 was  
123 digested by *Eco*RI and *Spe*I, cloned into the *Eco*RI–*Xho*I sites of pPICZ $\alpha$ A, and designated  
124 as pPICZ $\alpha$ A-CWH41 for the production of ScGI.

125

126         *Production and purification of SpGIIa. E. coli* BL21-CodonPlus (DE3)-RIL cells were  
127 transformed by pET23d-gls2. Transformants were selected on an LB agar plate (5 g/L NaCl,  
128 10 g/L bacto tryptone, 5 g/L bacto yeast extract and 15 g/L agar), supplemented with 50 mg/L  
129 ampicillin and 30 mg/L chloramphenicol. A transformant was grown in 40 mL of LB liquid  
130 medium with 50 mg/L ampicillin and 30 mg/L chloramphenicol at 30°C overnight. The  
131 resultant 30 mL of overnight LB-culture was inoculated into TB medium (3 L; 12 g/L bacto  
132 tryptone, 24 g/L bacto yeast extract, 0.4% (v/v) glycerol, 170 mM KH<sub>2</sub>PO<sub>4</sub> and 720 mM  
133 K<sub>2</sub>HPO<sub>4</sub>) supplemented with 50 mg/L ampicillin and cell culturing was continued at 37°C.  
134 When the OD<sub>600</sub> reached 0.7, the culture broth was cooled on ice for 30 min. Induction of the  
135 culture was achieved at 12°C for 48 h without the addition of isopropyl β-  
136 thiogalactopyranoside (IPTG). Bacterial cells, harvested by centrifugation (11,600 × g, 4°C,  
137 10 min), were suspended in 150 mL of 20 mM sodium phosphate buffer (pH 7.5) containing  
138 10% (v/v) glycerol (buffer-A) and disrupted by sonication. The cell-free extract, obtained by  
139 centrifugation (9,600 × g, 4°C, 10 min), was applied to a Co-chelating Sepharose Fast Flow  
140 column (1.5 cm I.D. × 4 cm, GE Healthcare, Buckinghamshire, United Kingdom) equilibrated  
141 with buffer-A containing 0.5 M NaCl (buffer-B). After thorough washing with buffer-B and  
142 10 mM imidazole-containing buffer-B in this order, the adsorbed protein was eluted with a  
143 linear gradient of imidazole from 10 to 200 mM in buffer-B. The active fractions were loaded  
144 on to a Bio-Gel P6 fine column (3 cm I.D. × 28 cm, Bio-Rad, Richmond, CA) equilibrated  
145 with buffer-A. The desalted sample was then loaded onto a DEAE-Sepharose Fast Flow  
146 column (2.6 cm I.D. × 8.5 cm, GE Healthcare) equilibrated with buffer-A. After washing with  
147 buffer-A, the adsorbed protein was eluted with a linear gradient of NaCl from 0 to 1.0 M in  
148 buffer-A. The active fractions, desalted by the aforementioned procedure using Bio-Gel P6,  
149 were subjected to a second DEAE-Sepharose Fast Flow column chromatography (1.5 cm I.D.



150 × 6 cm) step. The adsorbed protein was eluted isocratically with 65 mM NaCl in buffer-A.  
151 The active fractions were pooled and desalted by Bio-Gel P6 using buffer-A. The purity of  
152 the protein was analyzed by SDS-PAGE. The concentration of the purified protein was  
153 estimated by amino acid analysis of the protein hydrolysate (6 M HCl, 110°C, 24 h) using  
154 JLC-500/V (JOEL, Tokyo, Japan) equipped with a ninhydrin-detection system. The extinction  
155 coefficient of 1 mg/mL purified SpGII $\alpha$  at 280 nm was 2.27.

156

157 *Production and purification of ScGI.* Transformation of *P. pastoris* GS115 was performed  
158 as described by Lin-Cereghino *et al.*<sup>19)</sup> pPICZ $\alpha$ A-CWH41A was linearized with *SacI* and  
159 introduced into *P. pastoris* cells by electroporation. Transformants were selected on YPDSZ  
160 agar plates (10 g/L bacto yeast extract, 20 g/L bacto peptone, 2 g/L glucose, 1 M sorbitol, 100  
161 mg/L Zeocin and 15 g/L agar). The selected transformant was grown in BMGY medium [3L;  
162 10 g/L bacto yeast extract, 20 g/L bacto peptone, 3.4 g/L yeast nitrogen base without amino  
163 acids and ammonium sulfate, 10 g/L ammonium sulfate, 0.1 M potassium phosphate buffer  
164 (pH 6.0), 10 g/L glycerol and 0.4 mg/L biotin] at 30°C overnight. The cells collected by  
165 centrifugation at 4°C for 10 min (3,000 × g) were resuspended in 500 mL of BMMY medium  
166 that contains 1% (v/v) methanol instead of the glycerol of BMGY and incubated at 22°C for  
167 96 h under vigorous shaking. One hundredth of the culture volume of methanol was added  
168 every 24 h. The supernatant was removed by centrifugation (11,600 × g, 4°C, 10 min) and its  
169 pH was adjusted to 7.5 by addition of 1 M NaOH with stirring. Debris were removed by  
170 centrifugation (11,600 × g, 4°C, 10 min) and the recovered supernatant was loaded onto a Ni-  
171 chelating Sepharose Fast Flow column (1.5 cm I.D. × 5 cm) equilibrated with 50 mM sodium  
172 phosphate buffer (pH 7.5) containing 0.5 M NaCl (buffer-C). After washing with buffer-C  
173 and then 5 mM imidazole-containing buffer-C, the adsorbed protein was eluted with 200 mM  
174 imidazole in buffer-C. The fractions containing purified ScGI, which was determined by SDS-

175 PAGE, were dialyzed against 20 mM potassium phosphate buffer (pH 6.8) containing 0.1 M  
176 NaCl and concentrated using Centriprep YM-50 centrifugal filter units (Novagen-Merck  
177 Millipore).

178

179 *Standard enzyme assay.* The activity of SpGII $\alpha$  was determined by measuring the  
180 increase of *p*-nitrophenol during hydrolysis of pNPG. A reaction mixture (50  $\mu$ L) consisting  
181 of an appropriate concentration of SpGII $\alpha$ , 2 mM pNPG, 40 mM MES-NaOH buffer (pH 6.5),  
182 2% (v/v) glycerol and 0.2 mg/mL bovine serum albumin (BSA) was incubated at 30°C for 10  
183 min. The reaction was stopped by mixing with two volumes of 1 M sodium carbonate. The  
184 amount of *p*-nitrophenol released was measured by absorption at 400 nm in a 1-cm cuvette,  
185 using a molar extinction coefficient of 5,560 M<sup>-1</sup> cm<sup>-1</sup>. One unit of SpGII $\alpha$  activity was  
186 defined as the amount of enzyme that produced 1  $\mu$ mol *p*-nitrophenol per min under these  
187 conditions.

188

189 *Optimum pH and stability to pH and heat.* The optimum pH of the catalytic reaction was  
190 determined by measuring the hydrolytic rate at various pH values. The SpGII $\alpha$  concentration  
191 and buffer used were 8.2  $\mu$ g/mL and 80 mM Britton–Robinson buffer (pH 2.7–11.5),  
192 respectively. The other reaction conditions were the same as those of the standard assay  
193 method. For measurement of pH stability, SpGII $\alpha$  (82  $\mu$ g/mL) was incubated in 10-fold-  
194 diluted Britton–Robinson buffer (pH 3.3 to 10.5) containing 0.1% BSA and 10% (v/v)  
195 glycerol at 4°C for 24 h, followed by measurement of the residual activity under the standard  
196 assay conditions. The stable region was defined as the pH range exhibiting residual activity  
197 of > 90%. For measurement of thermal stability, SpGII $\alpha$  (2.7  $\mu$ g/mL) in 67 mM MES-NaOH  
198 buffer (pH 6.5) containing 0.1% BSA and 10% (v/v) glycerol was kept at 26 to 55°C for 15  
199 min, followed by measurement of their residual activities under the standard assay conditions.

200 The stable region was defined as the temperature range exhibiting residual activity of > 90%.

201

202 *Effect of additives on enzyme stability.* SpGII $\alpha$  in 20 mM HEPES-NaOH (pH 7.5) was  
203 incubated with NaCl (0.05, 0.2, or 0.5 M), CaCl<sub>2</sub> (0.05 or 0.2 M), EDTA·2Na (0.1, 0.5, or 1  
204 mM), glycerol [2, 10, or 20% (v/v)], or Triton X-100 [0.5 or 1% (v/v)] at 4°C. At the indicated  
205 time, an aliquot of the mixture was taken and diluted with 40 mM MES-NaOH (pH 6.5)  
206 containing 0.1% BSA and 10% (v/v) glycerol. The residual activity was evaluated by  
207 hydrolysis of 0.2% maltose at 30°C. The hydrolysis reaction was terminated by mixing with  
208 two volumes of 2 M Tris-HCl buffer (pH 7.0) and liberated glucose was measured with the  
209 Glucose C II-Test Wako (Wako Pure Chemical Industries).

210

211 *Effect of various salts on the enzyme reaction.* The enzyme reactions were performed in  
212 40 mM MES-NaOH (pH 6.5) containing 1.6  $\mu$ g/mL SpGII $\alpha$ , 0.2% maltose, 2% (v/v) glycerol  
213 and 0.2 mg/mL BSA at 30°C for 10 min by adding salt (0–40 mM KCl, MgCl<sub>2</sub>, or various  
214 sodium salts). The concentration of liberated glucose was measured, as described above.

215

216 *Kinetic parameters for hydrolysis of various substrates.* Kinetic parameters for  
217 hydrolysis of pNPG, nigerose, kojibiose and a series of maltooligosaccharides were  
218 calculated from the initial rates at various substrate concentrations by fitting to the Michaelis–  
219 Menten equation using KaleidaGraph 3.6J (Synergy Software, Reading, PA, USA). Substrate  
220 concentrations were as follows: 0.4–15 mM for pNPG, 0.5–10 mM for nigerose, 1–80 mM  
221 for kojibiose, 3.2–80 mM for maltose, 2.0–64 mM for maltotriose, 2.0–80 mM for  
222 maltotetraose and maltopentaose, 2.0–40 mM for maltohexaose and 0.8–40 mM for  
223 maltoheptaose. Since the  $K_m$  value for isomaltose was so large, its  $k_{cat}/K_m$  value was  
224 determined from the slope of Lineweaver-Burk plots at concentrations from 16 to 80 mM.

225 The amount of *p*-nitrophenol released from pNPG was measured by absorption at 400 nm, as  
226 described above. For other substrates, the liberated glucose was measured as described above.

227

228 *Measurement of the hydrolytic rates of G2M3-Dansyl and G1M3-Dansyl.* The hydrolytic  
229 rates for G2M3-Dansyl and G1M3-Dansyl, both of which were prepared as described  
230 previously,<sup>20,21)</sup> and nigerose were determined by measuring the liberated glucose  
231 concentration. A reaction mixture (180  $\mu$ L) consisting of SpGII $\alpha$  (0.35  $\mu$ g/mL for nigerose  
232 and G2M3-Dansyl, 1.8  $\mu$ g/mL for G1M3-Dansyl), 0.4 mM substrate, 40 mM MES-NaOH  
233 buffer (pH 6.5), 2% (v/v) glycerol and 0.2 mg/mL BSA was incubated at 30°C. At 5, 10, 15  
234 and 20 min, an aliquot of the reaction mixture was taken and heated at 100°C for 3 min to  
235 terminate the reaction. The glucose concentration was measured by high-performance anion  
236 exchange chromatography [Dionex ICS-3000 system with pulsed amperometric detection  
237 (Dionex/Thermo Fisher Scientific, Idstein, Germany)]. The analytical column (CarboPac PA1,  
238 4 mm I.D.  $\times$  250 mm, Dionex/Thermo Fisher Scientific) was equilibrated by 100 mM NaOH  
239 at a flow speed of 0.8 mL min<sup>-1</sup>. Separations were performed with the 6 min-linear gradient  
240 of 100–640 mM NaOH for nigerose and with the 42 min-linear gradient of 0–600 mM sodium  
241 acetate in 100 mM NaOH for dansyl oligosaccharides. The NaOH solution was prepared from  
242 super special grade 50% NaOH (Wako Pure Chemical Industries). Standards and samples  
243 contained 0.1 mM fructose as an internal reference. Peak areas and retention times of eluted  
244 carbohydrates were evaluated with the Chromeleon software (Dionex/Thermo Fisher  
245 Scientific). The concentration of glucose in each sample was calculated from its peak area  
246 using a calibration curve prepared from standard glucose and internal fructose.

247

248 *Detection of deglycosylation of pyridylaminated oligosaccharides.* A reaction mixture  
249 (100  $\mu$ L) consisting of SpGII $\alpha$  (1.04  $\mu$ g/mL), 0.4  $\mu$ M substrate (G1M9-PA or G3M9-PA), 40

250 mM MES-NaOH buffer (pH 6.5), 2% (v/v) glycerol and 0.2 mg/mL BSA was incubated at  
251 30°C. For ScGI-catalyzed hydrolysis of the outermost glucose residue of G3M9-PA, 2.1  
252 µg/mL ScGI was used under the same reaction conditions as SpGIIα. The reaction was  
253 terminated by incubation at 95°C for 5 min. The oligosaccharides were separated by high-  
254 performance liquid chromatography (HPLC) using an Asahipack NH2-50-4E column (4.6  
255 mm I.D. × 250 mm, Shodex, Tokyo, Japan) at 40°C. The elution was done at a flow speed of  
256 0.8 mL min<sup>-1</sup> with a linear gradient of acetonitrile from 68 to 34% in 0.3% ammonium acetate  
257 buffer (pH 7.0). Pyridylaminated oligosaccharides were monitored by the fluorescence signal  
258 (excitation wave length, 310 nm; emission wavelength, 380 nm) using a fluorescence detector  
259 FP-2020 Plus (Jasco, Tokyo, Japan).

260

## 261 **Results and discussion**

### 262 *Production and characterization of SpGIIα*

263 The expression conditions for obtaining soluble recombinant SpGIIα in *E. coli* were  
264 examined. The DNA coding for the mature SpGIIα was in-frame inserted into different  
265 expression plasmids (pET23d, pCold I, or pET41a) and enzyme production was tested using  
266 three different *E. coli* strains [Rosetta (DE3), BL21-CodonPlus (DE3)-RIL, or -RP]. In most  
267 expression systems tested, recombinant SpGIIα was produced as an insoluble form; however,  
268 the BL21-CodonPlus (DE3)-RIL strain transformed with the pET23d was the best  
269 combination for soluble protein production. Furthermore, cultivation in TB medium  
270 supplemented with 50 µg/mL ampicillin at 12°C without IPTG induction was also effective  
271 for production of soluble SpGIIα.

272 The induced cells cultivated under the optimum conditions for 48 h were disrupted in 20  
273 mM sodium phosphate buffer (pH 7.5) including 10% glycerol, and the crude extract obtained  
274 contained 11.5 U per 1 L culture. The presence of glycerol in both the purification and storage

275 buffers was essential for preventing SpGII $\alpha$  from inactivation, as described below.  
276 Recombinant SpGII $\alpha$  produced by *E. coli* was purified using cobalt-affinity and anion-  
277 exchange chromatographies. The final desalting column step yielded 1.8 mg of  
278 electrophoretically homogeneous SpGII $\alpha$  (Fig. 1) from 3 L of culture with specific activity  
279 of 4.0 U/mg.

280 Figure 2 shows the effects of various additives on the stability of SpGII $\alpha$ . The residual  
281 activity of SpGII $\alpha$  without any additive decreased to < 40% of the initial activity after 2 d  
282 (Fig. 2A), and to < 1% after 23 d (Figs. 2B, C). Inhibitory effect was observed when the  
283 protein was incubated with NaCl, CaCl<sub>2</sub> and Triton X-100 (Fig. 2A). In particular, addition  
284 of CaCl<sub>2</sub> and Triton X-100 induced substantially activity loss. Both glycerol and EDTA as  
285 additives improved the stability of recombinant SpGII $\alpha$  (Figs. 2B, C). It is hard to understand  
286 how EDTA contributes to the stability of SpGII $\alpha$ . It is anticipated that EDTA removes  
287 contaminating divalent ions such as the calcium ion, which adversely affects the SpGII $\alpha$   
288 stability. The addition of  $\geq$  10% (v/v) glycerol was more effective in stabilizing SpGII $\alpha$  than  
289 EDTA, with the enzyme maintaining > 90% activity after 92 d (Fig. 2C). Glycerol is known  
290 to induce protein compaction, reduce protein flexibility, stabilize specific partially unfolded  
291 intermediates and affect protein aggregation,<sup>22)</sup> resulting in its wide use as a protein stabilizer.  
292 Based on the effect of glycerol on protein stability, Vangenende *et al.* proposed that glycerol  
293 prevents protein aggregation thorough preferential interaction with hydrophobic surface  
294 regions.<sup>22)</sup> In nature, GII $\beta$  forms a heterodimer with GII $\alpha$ . Thus, glycerol was anticipated to  
295 affect the exposed dimer interface of GII $\beta$  lacking the GII $\alpha$  subunit, because generally an  
296 oligomer interface is hydrophobic. However, the three-dimensional structure of murine GII $\alpha$   
297 complexed with an N-terminal portion of GII $\beta$  showed that the interface area is not that  
298 hydrophobic,<sup>8)</sup> suggesting less hydrophobicity of the equivalent regions of SpGII $\alpha$ . Therefore,  
299 it is possible that SpGII $\alpha$  has other surface exposed hydrophobic regions where glycerol

300 interacts to prevent instability of the protein. Nonetheless, stabilization conditions found in  
301 this study allow us to perform purification and characterization of SpGII $\alpha$ .

302 The effects of various salts on the activity were investigated by measuring the initial  
303 hydrolytic velocity on maltose using 2% (v/v) glycerol. NaCl, NaH<sub>2</sub>PO<sub>4</sub>, Na<sub>2</sub>SO<sub>4</sub>, NaNO<sub>3</sub>,  
304 KCl, MgCl<sub>2</sub>, or EDTA·2Na with concentrations up to 40 mM did not affect activity, while the  
305 addition of 40 mM CaCl<sub>2</sub> decreased to 63% of the original initial velocity. The calcium ion  
306 should be harmful to both activity and stability of SpGII $\alpha$ . As shown in Fig. 2A, 50 mM CaCl<sub>2</sub>  
307 causes its inactivation within 2 d, which shows a negative effect of this salt on its stability.

308 The effects of pH and temperature on the activity were examined in the presence of 10%  
309 (v/v) glycerol. The pH optimum was 6.5 and SpGII $\alpha$  was stable between pH 6.2 and 9.1.  
310 SpGII $\alpha$  was thermally stable to 40°C with complete inactivation observed at 55°C (15 min  
311 treatment). In the absence of glycerol, this thermal stability was reduced to < 30% of the  
312 initial activity observed when incubated in the presence of glycerol for 15 min at 40°C.

313

#### 314 *Substrate specificity of SpGII $\alpha$ : substrates for GH31 $\alpha$ -glucosidase*

315 Substrate specificity of GII $\alpha$  is of interest, because this protein has a common ancestor  
316 with GH31  $\alpha$ -glucosidases, which can hydrolyze  $\alpha$ -(1→2)-,  $\alpha$ -(1→3)-,  $\alpha$ -(1→4)- and  $\alpha$ -  
317 (1→6)-glucosidic linkages.<sup>23–27</sup> By primarily exhibiting specificity to  $\alpha$ -(1→4)-glucosidic  
318 linkage, GH31  $\alpha$ -glucosidases are mostly linked with metabolic pathways of starch and  
319 maltooligosaccharides degradation.<sup>28</sup> While GII $\alpha$  plays a different role in biological  
320 processes when compared with that of GH31  $\alpha$ -glucosidases, both enzymes might display  
321 similar substrate specificities, because catalytic function of a protein is generally conserved  
322 during molecular evolution. Substrate specificity of SpGII $\alpha$  towards common substrates of  $\alpha$ -  
323 glucosidases was evaluated by determining kinetic parameters (Table 1). SpGII $\alpha$  hydrolyzed  
324 all substrates tested, proving broader specificity than ER-resident processing GI, which

325 recognizes the outermost  $\alpha$ -1,2-glucosyl residue in the *N*-glycan so strictly that kojibiose acts  
326 as an inhibitor.<sup>29,30)</sup> Among the disaccharides, nigerose was the best substrate with the highest  
327  $k_{\text{cat}}/K_{\text{m}}$  value (Table 1). The  $K_{\text{m}}$  values for maltose and kojibiose were around 10 times as large  
328 as that for nigerose, and that for isomaltose could not be obtained due to unsaturated curve in  
329  $s - v$  plots up to 80 mM isomaltose, indicating that SpGII $\alpha$  displays weaker binding to  $\alpha$ -  
330 (1 $\rightarrow$ 4)-,  $\alpha$ -(1 $\rightarrow$ 2)- and  $\alpha$ -(1 $\rightarrow$ 6)-glucosidic linkages. This specificity is similar to the GH31  
331  $\alpha$ -1,3-glucosidase, which hydrolyzes  $\alpha$ -(1 $\rightarrow$ 4)-,  $\alpha$ -(1 $\rightarrow$ 2)- and  $\alpha$ -(1 $\rightarrow$ 3)-glucosidic linkages  
332 together with weak specificity towards the  $\alpha$ -(1 $\rightarrow$ 6)-glucosidic linkage.<sup>31-33)</sup> This enzyme has  
333 been found in some microorganisms and is hypothesized to be involved in a metabolic  
334 pathway rather than the trimming of sugar chains.<sup>31-33)</sup> Hydrolysis of pNPG was characterized  
335 by low  $k_{\text{cat}}$  and  $K_{\text{m}}$  values, which are common features of the GH31  $\alpha$ -glucosidases and the  $\alpha$ -  
336 1,3-glucosidase.<sup>23-25,28,31,32)</sup> These results demonstrate that SpGII $\alpha$  conserves substrate  
337 specificity while its localization and physiological role are different. The higher  $k_{\text{cat}}/K_{\text{m}}$  value  
338 for maltose than that for malto-triose, -tetraose and -pentaose (Table 1) indicates that SpGII $\alpha$   
339 prefers maltose, and this observation is consistent with the structure of the active-site pocket  
340 of GII $\alpha$  being capable of accommodating only disaccharides.<sup>7,8)</sup> The  $k_{\text{cat}}/K_{\text{m}}$  values for malto-  
341 hexaose and -heptaose increased 3.0 to 5.2 times over -triose, -tetraose and -pentaose. The  
342 GH31 sugar beet  $\alpha$ -glucosidase possesses the machinery that accommodates long-chain  
343 substrates,<sup>34)</sup> but SpGII $\alpha$  has no equivalent element. Thus, it is difficult to explain the increase  
344 in specificity toward longer-chain substrates.

345

#### 346 *Substrate specificity of SpGII $\alpha$ : N-glycan-relating substrates*

347 We measured the hydrolytic rates on 0.4 mM G2M3-Dansyl and G1M3-Dansyl, which  
348 mimic arm A of *N*-glycan, together with 0.4 mM nigerose for comparison. SpGII $\alpha$  was able  
349 to hydrolyze the  $\alpha$ -glucosidic linkage in G2M3-Dansyl and G1M3-Dansyl with hydrolytic



350 rates of 1.23 and 0.274  $\mu\text{mol min}^{-1} \text{mg}^{-1}$ , respectively, although these values were slower than  
351 that of nigerose (2.42  $\mu\text{mol min}^{-1} \text{mg}^{-1}$ ). The difference in hydrolytic rates between G2M3-  
352 Dansyl and G1M3-Dansyl is in agreement with the observation that GII catalyzes the  
353 hydrolysis of the  $\alpha$ -Glu-(1 $\rightarrow$ 3)-Glc linkage (cleavage-1) faster than that of the  $\alpha$ -Glu-(1 $\rightarrow$ 3)-  
354 Man linkage (cleavage-2).<sup>35,36</sup> The difference in the catalytic rate between both cleavages  
355 was accounted for by binding of GII $\beta$  to mannose residues in arms B and C.<sup>35-37</sup> Alternatively,  
356 recent crystal structure analyses proposed that an interaction between OH-2 of a mannose  
357 residue and the carboxy group of the acid/base catalyst of GII $\alpha$  is responsible for the slow  
358 reaction rate of cleavage-2.<sup>7,8</sup> Our SpGII $\alpha$ , devoid of GII $\beta$ , shows cleavage-2, corroborating  
359 the latter explanation.

360 GII $\alpha$  without the GII $\beta$  is able to hydrolyze much smaller substrates, such as pNPG, but  
361 not able to deglycosylate G2M9 and G1M9. These distinct results are also reported as follows.  
362 Stigliano *et al.* demonstrated that SpGII $\alpha$  was able to degrade G2M9 and G1M9 *in vivo*.<sup>12</sup>  
363 GII $\alpha$  in *S. cerevisiae* catalyzes cleavage-1 but not cleavage-2.<sup>14</sup> GII $\alpha$  from *B. mori* weakly  
364 hydrolyzes G1M9 *in vitro*.<sup>15</sup> According to these observations, GII $\alpha$  does not seem to require  
365 GII $\beta$  to hydrolyze the  $\alpha$ -glucosidic linkages in *N*-glycan. We thus examined hydrolysis of  
366 G1M9-PA and G3M9-PA using the purified SpGII $\alpha$  to evaluate its hydrolytic ability toward  
367 *N*-glycan. SpGII $\alpha$  weakly but clearly catalyzed cleavage-2 to generate M9-PA from G1M9-  
368 PA (Fig. 3A). After 1 h of the reaction, the peak of M9-PA appeared, and then increased to  
369 the same level of G1M9-PA after the reaction had proceeded for 12 h. As shown in Fig. 3B,  
370 SpGII $\alpha$  cannot degrade G3M9-PA (Fig. 3B), which coincides with the general specificity of  
371 GII. Conversion from G3M9 to G2M9 is known to be catalyzed by GI, which removes the  
372 outermost  $\alpha$ -Glc-(1 $\rightarrow$ 2)-Glc linkage of G3M9. ScGI rapidly hydrolyzed G3M9-PA to produce  
373 G2M9-PA (Fig. 3C). Figure 3D shows the hydrolysis of G3M9-PA in the presence of SpGII $\alpha$   
374 and ScGI, which demonstrates that G2M9-PA, generated by the rapid reaction of ScGI until

375 1 h, is degraded to G1M9-PA and M9-PA at 12 h. These results indicate that the purified  
376 SpGII $\alpha$  catalyzes the trimming of glucose residues from G2M9-PA and G1M9-PA without the  
377 assistance of GII $\beta$ . Although the purified SpGII $\alpha$  certainly catalyzes cleavage-1 and -2, their  
378 reaction rates are not high (Figs. 3A, 3D). According to the result of Watanabe *et al.*,<sup>37)</sup> 50%  
379 conversion of 25  $\mu$ M G1M9 to M9 requires 45 min by a membrane fraction containing GII,  
380 even though the accurate concentration of GII was unknown. The present study provides a  
381 more quantitative analysis in which 9.6 nM SpGII $\alpha$  (1.0  $\mu$ g/mL SpGII $\alpha$ ) and a 12-h reaction  
382 yield approximately 50% conversion of 0.4  $\mu$ M G1M9 (Fig. 3A). The low hydrolysis of G1M9  
383 and G2M9 by SpGII $\alpha$  is probably because of insufficient binding energy for efficiently  
384 hydrolyzing these natural substrates, because SpGII $\alpha$  can only hold the small terminal moiety  
385 of the comparatively large structure of G1M9 or G2M9. The active-site pocket of GII $\alpha$ s has  
386 the gourd-shaped bilocular pocket, which can accommodate only disaccharides,<sup>7,8)</sup> and GII $\beta$   
387 would be necessary to stabilize the enzyme-substrate complex. Olson *et al.* demonstrates an  
388 importance of the MRH domain of GII $\beta$  to the hydrolytic activity of GII $\alpha$  through a  
389 recognition of arms B and C of the natural *N*-glycan.<sup>13)</sup> We need to direct our future studies  
390 to understanding the effect of GII $\beta$  on the catalytic properties including substrate recognition.

391

#### 392 **Author contributions**

393 Conceived and designed the experiments: M. Okuyama. Performed the experiments: M.  
394 Okuyama, M. Miyamoto, I. Matsuo, S. Iwamoto, R. Serizawa and M. Tanuma. Contributed  
395 reagents/materials/analysis tools: M. Ma, P Klahan and Y. Kumagai. Wrote the paper: M.  
396 Okuyama, T. Tagami and A. Kimura.

397

#### 398 **Disclosure statement**

399 No potential conflict of interest was reported by the authors.

400

401 **Acknowledgements**

402       We thank the staff of the Instrumental Analysis Division of the Creative Research  
403 Institution at Hokkaido University for the amino acid analysis, and Applied Microbiology  
404 Laboratory, Research Faculty of Agriculture, Hokkaido University for the supply of *S. pombe*  
405 AHU 3179. We also thank Dr. S. Fukiya of the Laboratory of Microbial Physiology, Research  
406 Faculty of Agriculture, Hokkaido University for the analysis of pyridylaminated  
407 oligosaccharides. This work was supported by JSPS KAKENHI Grant Numbers 22780082  
408 and 26450114.

409

410 **References**

- 411 1. Parodi AJ. Role of *N*-oligosaccharide endoplasmic reticulum processing reactions in  
412 glycoprotein folding and degradation. *Biochem. J.* 2000;348:1–13.
- 413 2. Ernst HA, Lo Leggio L, Willemoes M, et al. Structure of the *Sulfolobus solfataricus*  
414  $\alpha$ -glucosidase: Implications for domain conservation and substrate recognition in  
415 GH31. *J. Mol. Biol.* 2006;358:1106–1124.
- 416 3. Sim L, Quezada-Calvillo R, Sterchi EE, et al. Human intestinal maltase-  
417 glucoamylase: crystal structure of the N-terminal catalytic subunit and basis of  
418 inhibition and substrate specificity. *J. Mol. Biol.* 2008;375:782–792.
- 419 4. Tan K, Tesar C, Wilton R, et al. Novel  $\alpha$ -glucosidase from human gut microbiome:  
420 substrate specificities and their switch. *FASEB J.* 2010;24:3939–3949.
- 421 5. Ren L, Qin X, Cao X, et al. Structural insight into substrate specificity of human  
422 intestinal maltase-glucoamylase. *Protein Cell.* 2011;2:827–836.
- 423 6. Tagami T, Yamashita K, Okuyama M, et al. Molecular basis for the recognition of  
424 long-chain substrates by plant  $\alpha$ -glucosidases. *J. Biol. Chem.* 2013;288:19296–  
425 19303.
- 426 7. Satoh T, Toshimori T, Yan G, et al. Structural basis for two-step glucose trimming  
427 by glucosidase II involved in ER glycoprotein quality control. *Sci. Rep.*  
428 2016;6:20575.
- 429 8. Caputo AT, Alonzi DS, Marti L, et al. Structures of mammalian ER  $\alpha$ -glucosidase II  
430 capture the binding modes of broad-spectrum iminosugar antivirals. *Proc. Natl.*  
431 *Acad. Sci. USA.* 2016;113:E4630–E4638.
- 432 9. Pelletier MF, Marcil A, Sevigny G, et al. The heterodimeric structure of glucosidase  
433 II is required for its activity, solubility, and localization *in vivo*. *Glycobiology.*  
434 2000;10:815–827.

- 435 10. Trembl K, Meimaroglou D, Hentges A, et al. The  $\alpha$ - and  $\beta$ -subunits are required for  
436 expression of catalytic activity in the hetero-dimeric glucosidase II complex from  
437 human liver. *Glycobiology*. 2000;10:493–502.
- 438 11. Totani K, Ihara Y, Matsuo I, et al. Substrate specificity analysis of endoplasmic  
439 reticulum glucosidase II using synthetic high mannose-type glycans. *J. Biol. Chem.*  
440 2006;281:31502–31508. .
- 441 12. Stigliano ID, Caramelo JJ, Labriola CA, et al. Glucosidase II  $\beta$  subunit modulates *N*-  
442 glycan trimming in fission yeasts and mammals. *Mol. Biol. Cell*. 2009;20:3974–  
443 3984. .
- 444 13. Olson LJ, Orsi R, Peterson FC, et al. Crystal structure and functional analyses of the  
445 lectin domain of glucosidase II: Insights into oligomannose recognition.  
446 *Biochemistry*. 2015;54:4097–4111.
- 447 14. Wilkinson BM, Purswani J, Stirling CJ. Yeast GTB1 encodes a subunit of  
448 glucosidase II required for glycoprotein processing in the endoplasmic reticulum. *J.*  
449 *Biol. Chem*. 2006;281:6325–6333.
- 450 15. Watanabe S, Kakudo A, Ohta M, et al. Molecular cloning and characterization of the  
451  $\alpha$ -glucosidase II from *Bombyx mori* and *Spodoptera frugiperda*. *Insect Biochem.*  
452 *Mol. Biol*. 2013;43:319–327.
- 453 16. Petersen TN, Brunak S, von Heijne G, et al. SignalP 4.0: discriminating signal  
454 peptides from transmembrane regions. *Nat. Methods*. 2011;8:785–786.
- 455 17. Faridmoayer A, Scaman C. Truncations and functional carboxylic acid residues of  
456 yeast processing  $\alpha$ -glucosidase I. *Glycoconj. J*. 2007;24:429–437
- 457 18. Barker MK, Wilkinson BL, Faridmoayer A, et al. Production and crystallization of  
458 processing  $\alpha$ -glucosidase I: *Pichia pastoris* expression and a two-step purification  
459 toward structural determination. *Protein Expr. Purif*. 2011;79:96–101.

- 460 19. Lin-Cereghino J, Wong WW, Xiong S, et al. Condensed protocol for competent cell  
461 preparation and transformation of the methylotrophic yeast *Pichia pastoris*.  
462 Biotechniques. 2005;38:44–48.
- 463 20. Iino K, Iwamoto S, Kasahara Y, et al. Facile construction of 1,2-cis glucosidic  
464 linkage using sequential oxidation–reduction route for synthesis of an ER processing  
465  $\alpha$ -glucosidase I substrate, Tetrahedron Lett. 2012;53:4452–4456.
- 466 21. Iwamoto S, Kasahara Y, Kamei K, et al. Measurement of endo- $\alpha$ -mannosidase  
467 activity using a fluorescently labeled oligosaccharide derivative. Biosci. Biotechnol.  
468 Biochem. 2014;78:927–936.
- 469 22. Vagenende V, Yap MGS, Trout BL. Mechanisms of protein stabilization and  
470 prevention of protein aggregation by glycerol. Biochemistry. 2009;48:11084–11096.
- 471 23. Okuyama M, Tanimoto Y, Ito T, et al. Purification and characterization of the hyper-  
472 glycosylated extracellular  $\alpha$ -glucosidase from *Schizosaccharomyces pombe*. Enzyme  
473 Microb. Technol. 2005;37:472–480.
- 474 24. Nakai H, Ito T, Hayashi M, Kamiya K, et al. Multiple forms of  $\alpha$ -glucosidase in rice  
475 seeds (*Oryza sativa* L., var Nipponbare). Biochimie. 2007;89:49–62.
- 476 25. Sato F, Okuyama M, Nakai H, et al. Glucoamylase originating from *Schwanniomyces*  
477 *occidentalis* is a typical  $\alpha$ -glucosidase. Biosci. Biotechnol. Biochem. 2005;69:1905–  
478 1913.
- 479 26. Tagami T, Okuyama M, Nakai H, et al. Key aromatic residues at subsites + 2 and + 3  
480 of glycoside hydrolase family 31  $\alpha$ -glucosidase contribute to recognition of long-  
481 chain substrates. Biochim. Biophys. Acta. 2013;1834:329–335.
- 482 27. Saburi W, Okuyama M, Kumagai Y, et al. Biochemical properties and substrate  
483 recognition mechanism of GH31  $\alpha$ -glucosidase from *Bacillus* sp. AHU 2001 with  
484 broad substrate specificity. Biochimie. 2015;108:140–148.

- 485 28. Frandsen TP, Svensson B. Plant  $\alpha$ -glucosidases of the glycoside hydrolase family 31.  
486 Molecular properties, substrate specificity, reaction mechanism, and comparison  
487 with family members of different origin. *Plant. Mol. Biol.* 1998;37:1–13.
- 488 29. Dhanawansa R, Faridmoayer A, van der Merwe G, et al. Overexpression,  
489 purification, and partial characterization of *Saccharomyces cerevisiae* processing  $\alpha$ -  
490 glucosidase I. *Glycobiology.* 2002;12:229–234. .
- 491 30. Miyazaki T, Matsumoto Y, Matsuda K, et al. Heterologous expression and  
492 characterization of processing  $\alpha$ -glucosidase I from *Aspergillus brasiliensis* ATCC  
493 9642. *Glycoconj. J.* 2011;28:563–571.
- 494 31. Yamamoto T, Unno T, Watanabe Y, et al. Purification and characterization of  
495 *Acremonium implicatum*  $\alpha$ -glucosidase having regioselectivity for  $\alpha$ -1,3-glucosidic  
496 linkage. *Biochim. Biophys. Acta.* 2004;1700:189–198.
- 497 32. Kang M-S, Okuyama M, Mori H, et al. The first  $\alpha$ -1,3-glucosidase from bacterial  
498 origin belonging to glycoside hydrolase family 31. *Biochimie.* 209;91:1434–1442.
- 499 33. Song KM, Okuyama M, Kobayashi K, et al. Characterization of a glycoside  
500 hydrolase family 31  $\alpha$ -glucosidase involved in starch utilization in *Podospora*  
501 *anserina*. *Biosci. Biotechnol. Biochem.* 2013;77:2117–2124.
- 502 34. Tagami T, Yamashita K, Okuyama M, et al. Structural advantage of sugar beet  $\alpha$ -  
503 glucosidase to stabilize the Michaelis complex with long-chain substrate. *J. Biol.*  
504 *Chem.* 2015;290:1796–1803.
- 505 35. Kaushal GP, Pastuszak I, Hatanaka K, et al. Purification to homogeneity and  
506 properties of glucosidase II from mung bean seedlings and suspension-cultured  
507 soybean cells. *J. Biol. Chem.* 1990;265:16271–16279.
- 508 36. Totani K, Ihara Y, Matsuo I, et al. Effects of macromolecular crowding on  
509 glycoprotein processing enzymes. *J. Am. Chem. Soc.* 2008;130:2101–2107.

- 510 37. Watanabe T, Totani K, Matsuo I, et al. Genetic analysis of glucosidase II  $\beta$ -subunit  
511 in trimming of high-mannose-type glycans. *Glycobiology*. 2009;19:834–840.
- 512 38. Deprez P, Gautschi M, Helenius A. More than one glycan is needed for ER  
513 glucosidase II to allow entry of glycoproteins into the calnexin/calreticulin cycle.  
514 *Mol. Cell*. 2005;19:183–195.  
515



516 **Table**

517 Table 1. Kinetic parameters of SpGII $\alpha$  hydrolysis of GH31  $\alpha$ -glucosidase substrates.

Substrate	$K_m$ (mM)	$k_{cat}$ (sec $^{-1}$ )	$k_{cat}/K_m$ (sec $^{-1}$ M $^{-1}$ )
<i>p</i> NPG	3.62 $\pm$ 0.02	0.0150 $\pm$ 0.0001	4.15
Nigerose	2.13 $\pm$ 0.06	0.102 $\pm$ 0.001	48.1
Kojibiose	21.0 $\pm$ 1.6	0.0575 $\pm$ 0.001	2.75
Isomaltose	N.D.	N.D.	0.014 $\pm$ 0.007
Maltose	18.0 $\pm$ 0.1	0.241 $\pm$ 0.007	13.4
Maltotriose	16.0 $\pm$ 0.3	0.0343 $\pm$ 0.0001	2.15
Maltotetraose	28.5 $\pm$ 2.5	0.0477 $\pm$ 0.0012	1.68
Maltopentaose	26.7 $\pm$ 0.2	0.0367 $\pm$ 0.0004	1.38
Maltohexaose	15.3 $\pm$ 0.6	0.109 $\pm$ 0.001	7.15
Maltoheptaose	15.0 $\pm$ 0.2	0.0965 $\pm$ 0.0007	6.43

518 N.D.: Values could not be determined because *s-v* plots were not saturated.

519 **Figure captions**

520 Fig. 1. Expression and purification of recombinant SpGII $\alpha$ .

521 Notes: Expression and purification of GII $\alpha$  were analyzed by 10% SDS–PAGE. Lane 1,  
522 IPTG-induced whole *E. coli* cells harboring pET23d-gls2; lane 2, supernatant from cell lysate  
523 of lane 1; lane 3, eluate from Co<sup>2+</sup> affinity chromatography; lane 4, Bio-Gel P6  
524 chromatography (1st); lane 5, anion exchange chromatography (1st); lane 6, Bio-Gel P6  
525 chromatography (2nd); lane 7, anion exchange chromatography (2nd); lane 8, Bio-Gel P6  
526 chromatography (3rd); lane M, marker proteins with molecular masses (kDa) shown at the  
527 side.

528

529 Fig. 2. Effect of additives on long-term stability of SpGII $\alpha$ .

530 Notes: (A) Residual activity of GII $\alpha$  was measured after incubation with various  
531 additives at 4 °C for 2 days. (B) Time course of residual activity of GII $\alpha$  in the presence of  
532 0.1 mM ( $\circ$ ), 0.5 mM ( $\blacksquare$ ) and 1 mM ( $\square$ ) EDTA·2Na. (C) Time course of residual activity of  
533 GII $\alpha$  in the presence of 2% ( $\circ$ ), 10% ( $\blacksquare$ ), and 20% ( $\square$ ) glycerol. The residual activity without  
534 any additives is represented by closed circles ( $\bullet$ ) in both (B) and (C).

535

536 Fig. 3. HPLC analysis of the hydrolysates of (A) G1M9 by SpGII $\alpha$ , (B) G3M9 by SpGII $\alpha$ ,  
537 (C) G3M9 by ScGI, and (D) G3M9 by ScGI and SpGII $\alpha$ .

538 Notes: The reaction mixture samples were taken at 0, 1 and 12 h and were analyzed by  
539 HPLC. Symbol used for the structure formulae:  $\blacktriangle$ , glucose;  $\circ$ , mannose; and  $\blacksquare$ , *N*-  
540 acetylglucosamine.

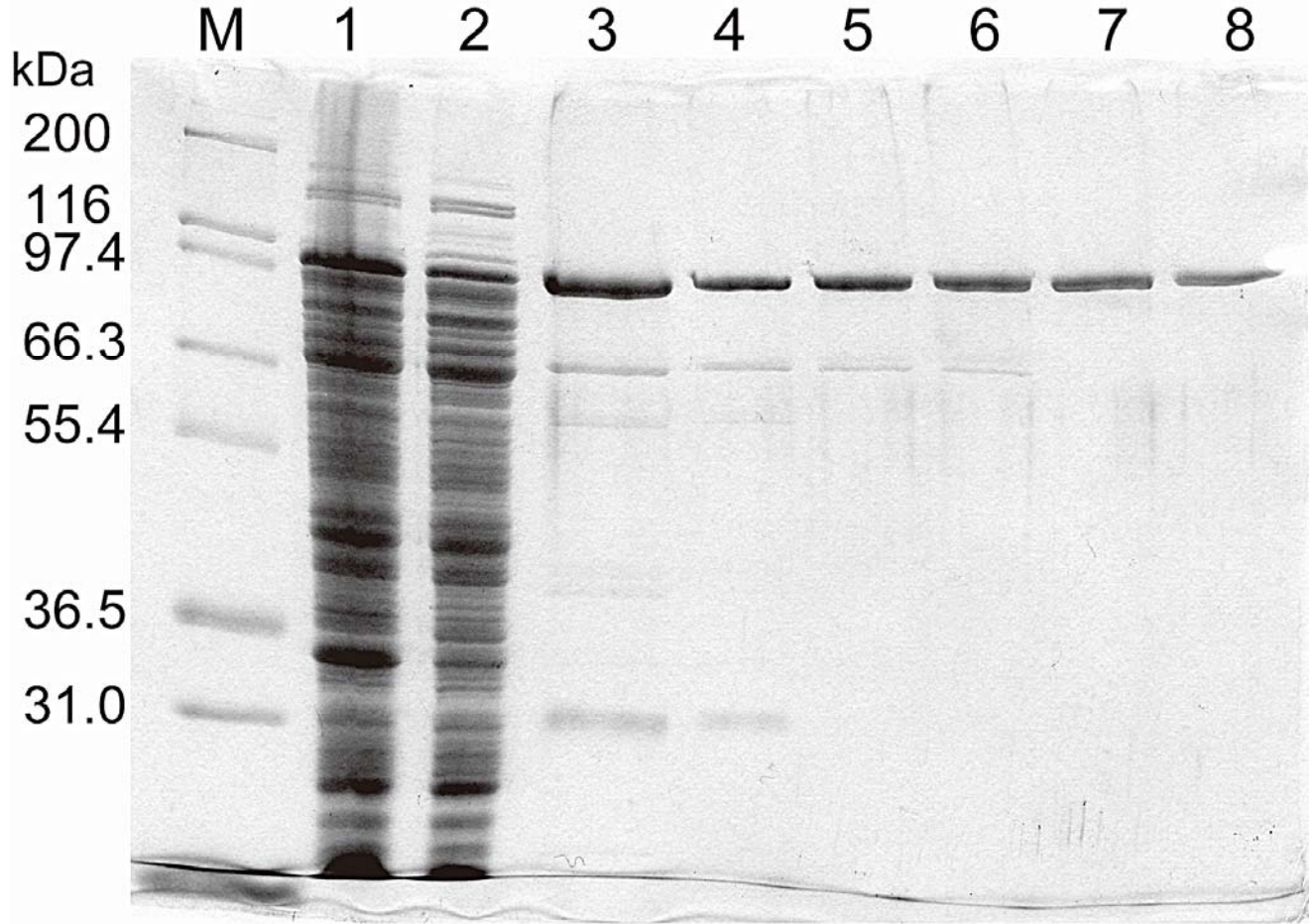


Figure 1. Okuyama et al

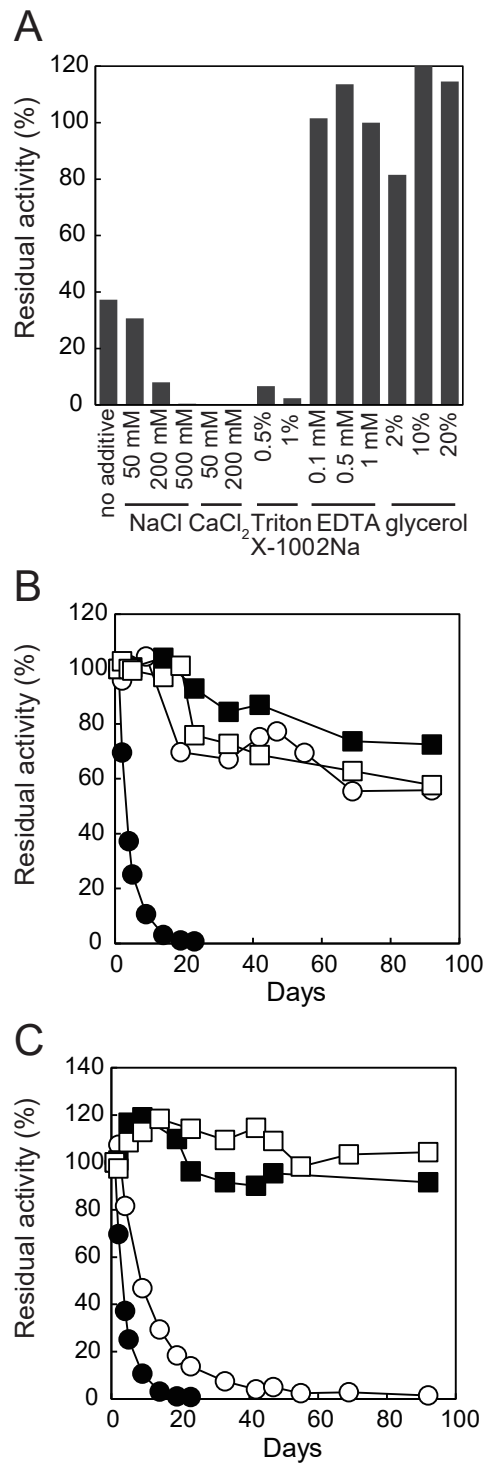


Figure 2. Okuyama et al

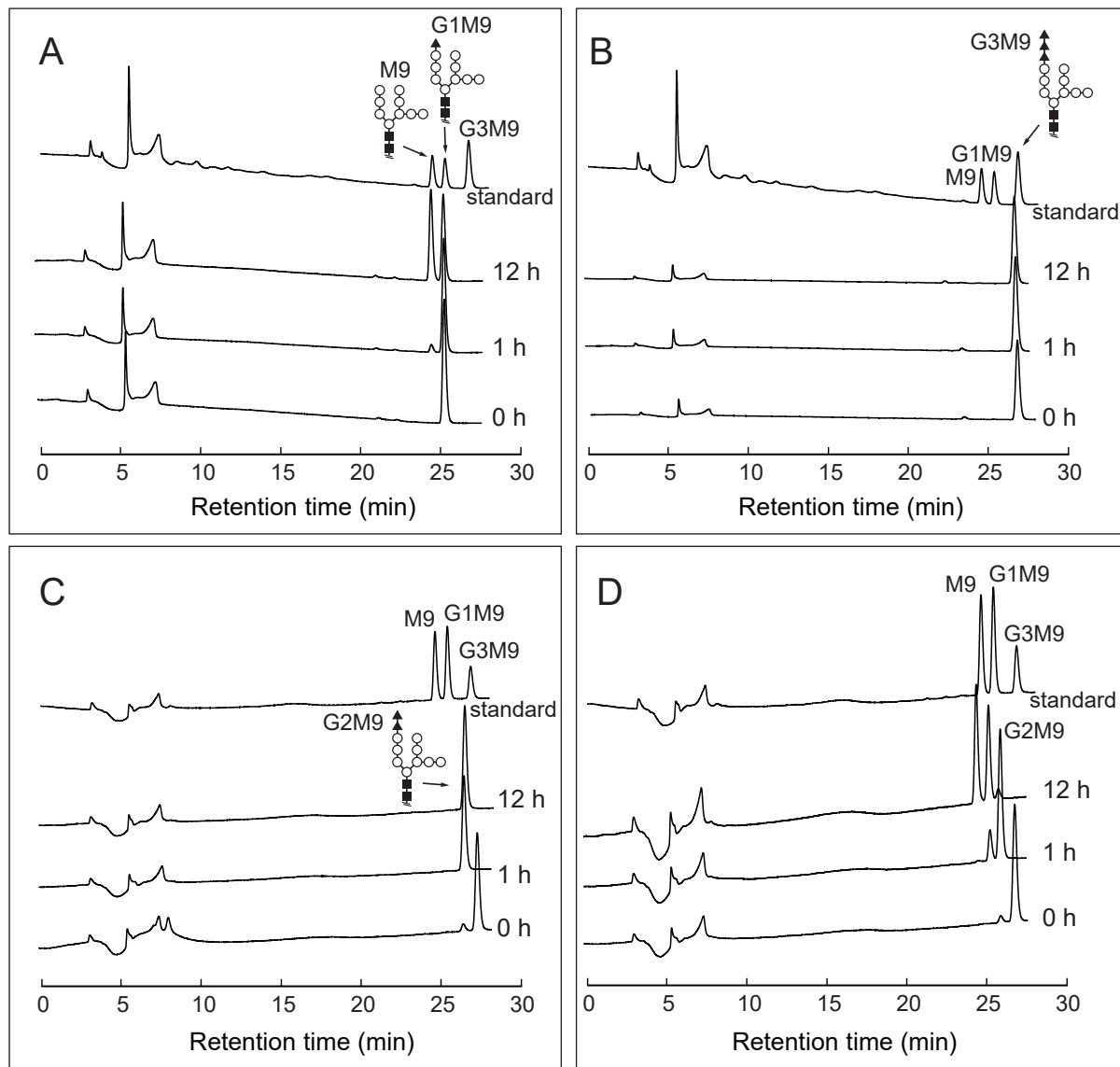


Figure 3. Okuyama et al